



Density functional study of acrolein adsorption on Pt (111)



S. Pirillo^a, I. López-Corral^a, E. Germán^b, A. Juan^{b,*}

^a Instituto de Química del Sur (INQUISUR, UNS–CONICET) and Departamento de Química, Universidad Nacional del Sur, Av. Alem 1253, B8000CPB Bahía Blanca, Argentina

^b Instituto de Física del Sur (IFISUR, UNS–CONICET) and Departamento de Física, Universidad Nacional del Sur, Av. Alem 1253, B8000CPB Bahía Blanca, Argentina

ARTICLE INFO

Article history:

Received 5 April 2013

Received in revised form

16 May 2013

Accepted 24 June 2013

Keywords:

Acrolein

Pt (111)

Adsorption

DFT

Bonding

ABSTRACT

The electronic structure and bonding of acrolein (propenal) adsorption on Pt (111) were studied by density functional calculations (DFT). We optimized different adsorption configurations on the surface using the VASP code. The energetic study indicates that acrolein trans isomers are less stable on the Pt surface than cis configurations, which have a similar stability in all cases. We found that the inclusion of Van der Waals (vdW) corrections does not change the obtained adsorption geometries or preferential sites relative energies. We also analyzed the evolution of the chemical bonding changes in the adsorbate and the metal surface by crystal orbital overlap population (COOP) and overlap population (OP) analysis of selected bonds. Except for the η_1 configuration, the adsorption of acrolein on the surface is mainly due to the formation of C–Pt bonds. We also found that the acrolein C p_z orbital, perpendicular to the surface, play an important role in the adsorption, as well as Pt p_z and d_z^2 orbitals, whose lobes are well oriented to overlap with the adsorbate orbitals.

© 2013 Elsevier Ltd. All rights reserved.

1. Introduction

The hydrogenation of α – β unsaturated aldehydes is an important reaction in a great number of fine-chemical processes. These molecules present adjacent C=C and C=O double bonds in conjugation. The most interesting product of hydrogenation is the unsaturated alcohol obtained by selective hydrogenation of the C=O bond, in competition with the formation of the saturated aldehyde by C=C bond hydrogenation [1–5]. Many experimental studies have been dedicated to the search of catalysts able to selectively hydrogenate such aldehydes. Among them, platinum-based catalysts have been widely studied [2,5,6].

The design of new catalysts requires knowledge of the adsorption modes of the α – β unsaturated aldehydes and the nature of the preferred adsorption sites [7]. Since each double bond can interact – separately or in combination – with the metal atoms, α – β unsaturated aldehydes present several possible adsorption modes. Quantum chemical calculations are a useful tool to explore all the possible adsorption structures and to determine the most stable geometries. Delbecq and Sauter performed both semi-empirical (extended Hückel) [8] as density functional theory (DFT) [7] calculations for acrolein (propenal) and other α – β unsaturated

aldehydes on different Pt surfaces. These authors considered several adsorption modes according to the possible interaction of acrolein C=C and/or C=O bonds with the surface. They found that the η_3 -cis form is the most stable configuration adsorbed through its C=C bond, with a secondary interaction between the oxygen atom and the surface. Loffreda et al. performed total energy calculations and determined the most stable chemisorptions sites for acrolein/Pt (111) [9]. These authors reported DFT optimized geometries for various adsorption sites as a function of acrolein surface coverage, and found again that the η_3 -cis form is a very stable configuration for a wide coverage range.

In a previous article [10] we studied the evolution of the chemical bond during the adsorption of acrolein on a Pt (111) surface, considering several possible interaction configurations using geometries from previous calculations [7,9]. In the present study we performed more accurate DFT total energy calculations including Van der Waals (vdW) dispersion forces and a new geometry optimization. The electronic structure is analyzed using the concept of density of states (DOS) and the bonding evolution is followed by crystal orbital overlap population (COOP) curves.

2. Methodology

The energy calculations were carried out using the Vienna Ab-initio Simulation Package (VASP) code [11,12] within the framework of the generalized gradient approximation of the

* Corresponding author.

E-mail address: cajuan@uns.edu.ar (A. Juan).

density functional theory (GGA–DFT), with the exchange–correlation functional of Perdew–Wang 91. Additional calculations were performed to take into account dispersion forces. We included the semi-empirical Van der Waals correction as described by Grimme [13] using the default parameters for H, C and O, while those for Pt were fixed at the values $R_{vdW} = 12 \text{ \AA}$, $d = 20 \text{ \AA}$, $C_6 = 1.75$, and $R_{Pt} = 1.452 \text{ \AA}$. In all cases, the cutoff energy employed was 400 eV and it was considered an $8 \times 8 \times 1$ Monkhorst–Pack k -point grid for sampling the Brillouin zone [14]. During the ionic relaxation process, the forces acting on the ions were calculated using the Hellmann–Feynman theorem, including the Harris–Foulkes corrections [15].

The Pt (111) surface was modeled by a periodic slab consisting of 45 atoms distributed in five layers with a lattice parameter of 3.92 Å. The acrolein molecule was adsorbed on one side of the slab, yielding a low coverage of 1/9 monolayer (see Fig. 1). A vacuum region of 15 Å was considered to avoid interaction between the periodic images. According to previous calculations [7,9], seven bonding configurations were analyzed on the Pt (111) surface: η_1 -trans, η_2 -cis, η_2 -trans, η_3 -cis, η_3 -trans, η_4 -cis and η_4 -trans. The adsorption energies have been calculated making the following total energy difference:

$$\Delta E_{\text{ads}} = E(\text{C}_3\text{H}_4\text{O}/\text{Pt}) - E(\text{C}_3\text{H}_4\text{O}) - E(\text{Pt})$$

where $E(\text{C}_3\text{H}_4\text{O}/\text{Pt})$, $E(\text{C}_3\text{H}_4\text{O})$ and $E(\text{Pt})$ are the adsorbed acrolein energy, the isolated acrolein energy and the bare slab energy, respectively.

After geometry optimization, we computed the acrolein and Pt (111) DOS curves, which constitute useful tools to reveal the most important adsorbate–substrate interactions. An implementation of the Bader’s method [16] developed by Henkelman et al. [17] was used. The evolution of chemical bonding was studied by COOP curves and overlap population (OP) belonging to selected atom pairs, using the Spanish Initiative for Electronic Simulations with Thousands of Atoms (SIESTA) [18,19]. The OP value is a measure of the degree of bonding between two specified atoms [20]. During this analysis, the system was divided into two fragments: adsorbate and surface [21].

3. Results and discussion

3.1. Geometric optimization

Table 1 shows the optimized geometries for acrolein adsorption on a Pt (111) surface using the Perdew–Wang 91 exchange

Table 1
DFT optimized geometries for acrolein adsorption on a Pt (111) surface.^a

	η_1 -trans	η_2 -cis	η_2 -trans	η_3 -cis	η_3 -trans	η_4 -cis	η_4 -trans
$d(\text{C1H1})$	1.11	1.11	1.13	1.10	1.13	1.10	1.13
$d(\text{C2H2})$	1.09	1.10	1.09	1.09	1.10	1.10	1.10
$d(\text{C3H3})$	1.09	1.09	1.09	1.09	1.10	1.09	1.09
$d(\text{C3H4})$	1.09	1.09	1.10	1.10	1.10	1.09	1.10
$d(\text{C1=O})$	1.24	1.23	1.22	1.28	1.22	1.30	1.23
$d(\text{C1–C2})$	1.45	1.49	1.49	1.45	1.50	1.44	1.48
$d(\text{C2=C3})$	1.34	1.49	1.49	1.48	1.50	1.48	1.50
$d(\text{Pt–C1})$		2.83	2.83	2.60	2.89	2.46	2.84
$d(\text{Pt–C2})$		2.14	2.14	2.19	2.14	2.19	2.15
$d(\text{Pt–C3})$		2.11	2.10	2.09	2.11	2.09	2.11
$d(\text{Pt–O})$	2.23	3.02	3.39	2.24	3.40	2.17	2.87
$\alpha(\text{C–C=O})$	118.5	123.9	126.0	123.5	126.0	122.8	126.2
$\alpha(\text{C=C–C})$	124.8	117.4	115.2	117.5	115.7	118.8	115.8
$\alpha(\text{O=C–H1})$	121.0	120.7	121.0	118.1	121.2	117.4	120.2
$\alpha(\text{C=C–H2})$	121.3	115.6	115.8	117.5	115.3	118.4	116.2
$\alpha(\text{C=C–H3})$	120.0	113.8	113.9	113.4	112.5	113.6	114.1
$\alpha(\text{C=C–H4})$	123.3	113.0	114.1	113.2	114.3	112.6	113.4
$\alpha(\text{CH3H4})$	116.7	113.2	111.7	112.5	112.2	112.9	111.6

^a Distances are expressed in Å, and bond angles in degrees (°). See Fig. 1 for atom labeling.

correlation functional. The initial adsorption configurations, proposed by Loffreda et al. [9] (on the left side), and the final geometries obtained in this work (on the right side) are shown in Fig. 2. The three adsorbed trans configurations (η_2 , η_3 and η_4 -trans) are very similar, and they present the characteristic geometry of the η_2 -trans interaction. In effect, Table 1 shows that the η_2 , η_3 and η_4 -trans adsorption modes have very similar final interatomic distances and bonding angles. However, in the η_4 -trans configuration the Pt–O distance is shorter (15.3%) than in the other two trans conformers. On the other hand, the η_2 , η_3 and η_4 -cis modes present different final geometries when we compare them with initial data in [9], as can be seen in Table 1 and Fig. 2.

Table 2 compares our computed adsorption energy values with those previously reported by Delbecq and Sautet [7]. The η_2 , η_3 and η_4 -trans adsorption modes have comparable adsorption energy values, between –24.3 and –26.2 kcal/mol, while the three cis conformations studied have almost the same energy value (\sim –29.3 kcal/mol). The η_1 -trans configuration has the lowest adsorption energy. These results indicate that the trans isomers are less stable than the cis ones, which is in agreement with experimental observations. Reflection–absorption infrared (RAIRS) spectroscopy measurements suggest that acrolein isomerizes from trans to cis conformation when is adsorbed [6]. The similar energy

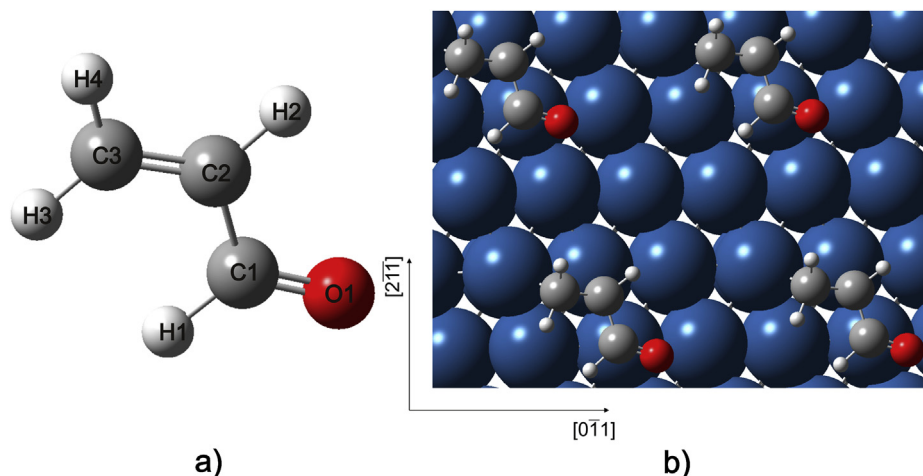


Fig. 1. (a) Isolated acrolein geometry and numbering. (b) Top view of acrolein adsorbed on Pt (111).

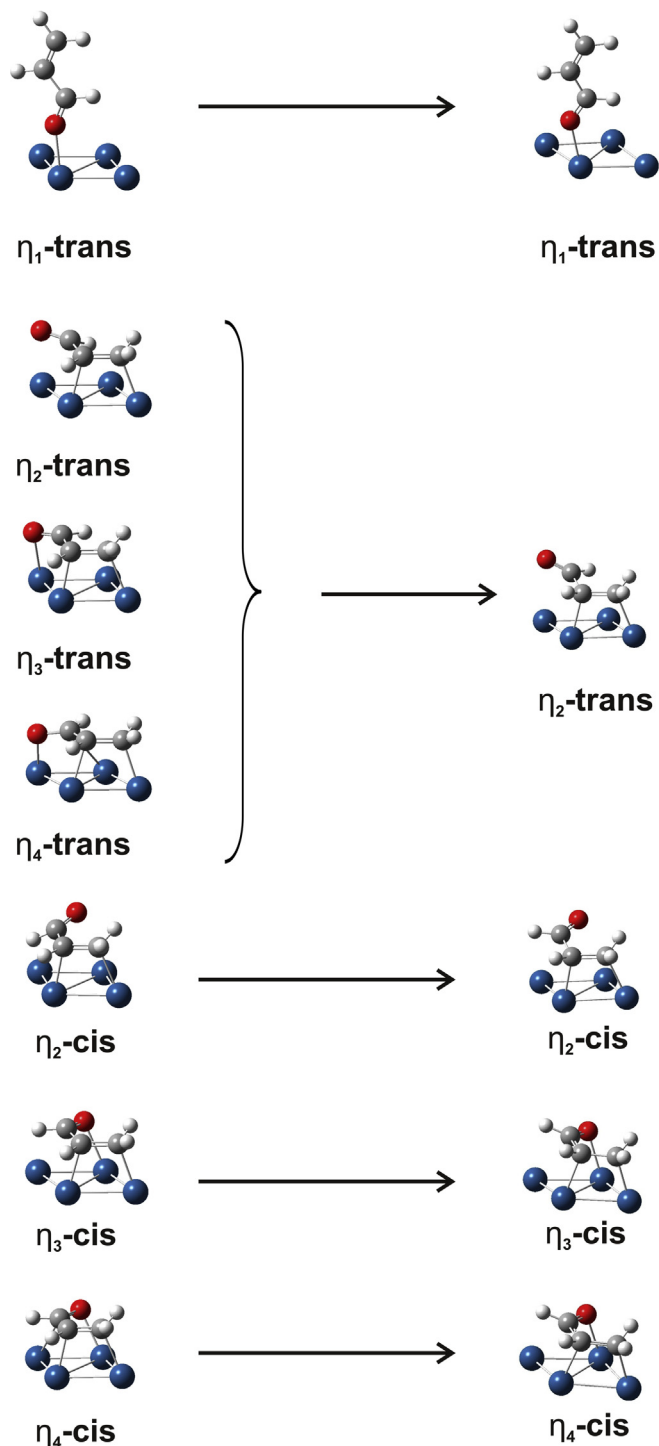


Fig. 2. Different adsorption modes for acrolein on a Pt (111) surface. Left: Initial adsorption configurations, proposed by Loffreda et al. [9]. Right: Final geometries obtained in this work.

value for the η_2 , η_3 and η_4 -trans adsorption configurations can be understood because after geometry relaxation on the Pt surface, the final structure is very similar in these cases, although for the η_4 -trans form the Pt–O distance is shorter. The similarities between the trans or the cis modes will be explained in detail in Section 3.2, though bonding analysis. Table 2 also includes the energy values reported by Delbecq and Sautet [7] indicating that the most stable adsorption mode is the η_3 -cis. Our results are in agreement with

Table 2

Adsorption energy values belonging to the different adsorption modes for acrolein adsorbed on Pt (111).

Adsorption mode	ΔE_{ads} (kcal/mol)	ΔE_{ads} (kcal/mol) ^a
η_1 -trans	–5.0	–6.0
η_2 -cis	–29.0	–21.7
η_2 -trans	–26.2	–21.8
η_3 -cis	–29.0	–23.6
η_3 -trans	–26.1	–
η_4 -cis	–30.0	–20.2
η_4 -trans	–24.3	–23.2

^a Reference [7].

this finding, although all cis conformers have a similar stability on the surface. These differences can be explained because our calculation uses a higher k -point set.

We also performed the same calculation considering vdW dispersion forces. The concerted effect of covalency and vdW bonding for benzene adsorbed on metals (including Pt) was recently analyzed by Liu et al. [22]. The authors demonstrated that the inclusion of vdW interactions increases the binding, and results in a much better agreement with experimental adsorption energies in both chemisorbed (Benzene/Pt) and physisorbed (Benzene/Au) systems. However, the changes in bond distances are less than 1% in chemisorbed benzene being higher in the case of Au (>20%). In the case of water adsorption on metals [23], the increase in the adsorption energy comes almost exclusively from an increased water–metal interaction, while the explicit consideration of vdW dispersion forces does not alter the relative stabilities of structures predicted by PBE. In addition, the adsorption sites remain unchanged and adsorption geometries (water–metal bond and water H-bond lengths) are very similar to calculations that do not include vdW corrections.

In the case of acrolein/Pt (111) the inclusion of vdW corrections to the energy produces larger adsorption energies (with a correction of about 4 kJ mol^{-1}) but predicted the same adsorption sites and very similar bond distances while the relative values of energies remain unaltered. Similar results were reported by Ferullo et al. [24] modeling acrolein on Ag (111) and by Hanke et al. [25] in the case of weakly chemisorbed ethene adsorbed on low-index Cu surfaces. As mentioned by Tonigold and Grob [26], a pure DFT–GGA approach leads to adsorption energies that are underestimated compared to experimental results. Adding dispersion corrections causes an overbinding to the metal substrate. Recent DFT calculations for acrolein hydrogenation on Pt do not include vdW corrections [27,28]. Unfortunately it is impossible to check for the effect of vdW corrections to the energy because there is not experimental data available in the open literature for the heat of adsorption of acrolein on Pt surfaces. According to this, the geometries used in the next were those computed with DFT–GGA approach with no vdW corrections added.

3.2. Bonding analysis

After geometry optimization, we examined the evolution of the chemical bonding in the preferential adsorbate–surface configurations. Table 3 lists the atom–atom OP values that play an important role during the acrolein adsorption. The η_1 -trans adsorption mode presents a single interaction with the surface through the O atom, with an =O–Pt OP value of 0.22. During this adsorption process the acrolein bonds are almost not weakened, because the molecule does not interact with the metallic surface though the C=C or C=O bonds. Simultaneously, the OP value belonging to the Pt–Pt bonds that interact with the O atom decreases only 5.6%. On the other

Table 3
Percent change in OP and OP values for bonds formed after acrolein adsorption.

Bond	%OP						
	η_1 -trans	η_2 -cis	η_2 -trans	η_3 -cis	η_3 -trans	η_4 -cis	η_4 -trans
Pt–Pt	–5.6	–16.7	–15.7	–18.5	–15.1	–20.8	–15.7
C=C	1.4	–1.8	–4.5	4.0	–5.1	5.0	–3.6
C=C	–1.4	–34.0	–34.7	–33.4	–35.0	–32.9	–34.5
C=O	0.1	–3.4	–0.2	–12.7	–0.5	–17.0	–2.6

Bond	OP values						
	η_1 -trans	η_2 -cis	η_2 -trans	η_3 -cis	η_3 -trans	η_4 -cis	η_4 -trans
–C–Pt	0.00	0.03	0.02	0.11	0.02	0.18	0.02
=C–Pt	0.00	0.44	0.45	0.37	0.45	0.34	0.44
=C–Pt	0.00	0.51	0.51	0.52	0.51	0.52	0.51
=O–Pt	0.22	0.00	0.00	0.18	0.00	0.21	0.00

hand, both η_2 -cis and η_2 -trans structures are stabilized by an interaction between their C=C bond and two Pt atoms. The O atom does not interact with the surface. This is evident in Table 3 because significant =C–Pt OP are developed and the weakening of the C=C and Pt–Pt bonds are important during the η_2 adsorptions (up to 34.7 and 16.7% respectively). In the η_3 configuration, both acrolein C=C bond and O atom interact with a surface Pt atom. The cis conformer presents a strong interaction with the surface, considering in Table 3 that important =C–Pt, –C–Pt and =O–Pt OP values are computed. At the same time, C=C, C=O and Pt–Pt overlaps decrease as a result of the noticeable adsorbate-surface interactions. In contrast, only =C–Pt interactions are developed in the η_3 -trans form, and the olefinic bond is notoriously weakened (about –35.0%). Therefore, we can conclude that the initial η_3 -trans geometry evolved to a η_2 -trans configuration, with only two bonds between the C=C bond and the Pt atoms. In line with this idea, similar energy values were obtained for the η_3 and η_2 -trans modes (see Table 2).

Table 3 also shows that important –C–Pt and =O–Pt OP values are developed in the η_4 -cis configuration, so both C=C as C=O bonds interact with the surface in a flat adsorption geometry. The η_4 -cis isomer presents the largest –C–Pt OP formation value (0.18), which indicates that the acrolein molecule interacts strongly with the Pt atoms through its saturated C (C1). Moreover, this configuration presents a high =O–Pt OP value and the largest weakening for the C=O and Pt–Pt bonds (–17.0 and –20.8%, respectively). The =C–Pt OP value and the C=C %OP reduction are similar to those of the other geometries. In the case of η_4 configuration only =C–Pt overlaps is developed and neither –C–Pt nor =O–Pt interactions are detected. In this case only the C=C bond is strongly weakened. This behavior indicates that the initial η_4 -trans configuration evolves to a final η_2 -trans geometry, like in the η_3 -trans adsorption process. The similar energy values obtained for the η_2 , η_3 y η_4 -trans modes support this idea (see Table 2). It must be remembered that the η_2 , η_3 y η_4 -cis adsorption modes present practically the same energy value (see Section 3.1). Table 3 reveals that the =C–Pt, –C–Pt and =O–Pt OP are different in these three configurations. This fact could be explained taking into account that in these geometries the different interactions are compensated, so a similar total overlap is achieved.

To shed more insight into the bonding evolution during acrolein adsorption, we evaluated COOP curves in the most stable configurations. COOP curves corresponding to the =C–Pt bond in the η_4 -cis mode obtained in this study and the η_3 -cis form proposed by Loffreda et al. [9] are shown in Fig. 3(a) and (b), respectively. Bonding states are located below the Fermi level in both adsorption configurations, between –1 and –6.5 eV. However, our η_4 -cis adsorption form an antibonding peak appears at approximately –0.7 eV, while

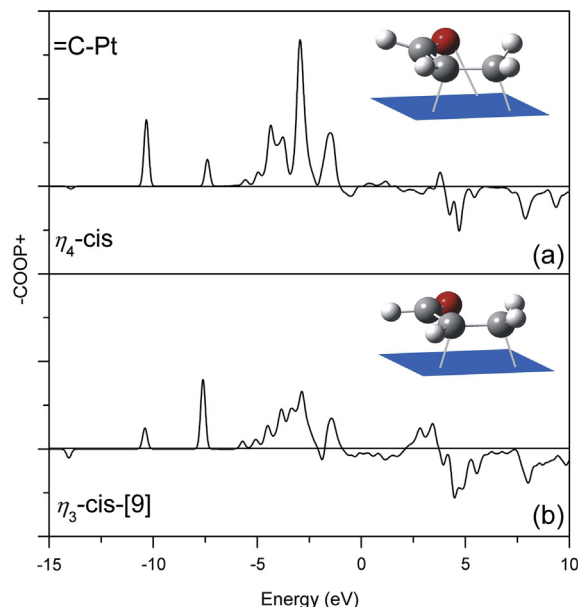


Fig. 3. Crystal orbital overlap population (COOP) curves of =C–Pt formed bond in selected configurations during adsorption process of acrolein on a Pt (111) surface. (a) η_4 -cis obtained in the present study. (b) η_3 -cis proposed by Loffreda et al. [9].

a strong antibonding peak can be observed at about –1.5 eV in the analyzed η_3 -cis geometry. In the region between –1.25 and –6.2 eV the differences are more evident because the η_4 -cis adsorption configuration presents stronger and narrower peaks than that of the η_3 -cis structure. Both configurations have a bonding peak at approximately –10.5 eV, which is more defined and intense in the η_4 -cis adsorption mode. As a result of bonding and antibonding interactions, =C–Pt overlaps in our η_4 -cis conformer are stronger than those for the η_3 -cis form presented in reference [9], as can be seen in Table 3.

The COOP curves belonging to the C=C bond in our η_4 -cis and the η_3 -cis form obtained by Loffreda et al. [9] are compared in Fig. 4(a) and (b), respectively, with the isolated cis isomer. In the gas-phase, acrolein *s* and *p* orbitals present narrow peaks, but after adsorption are re-hybridized as a result of the interaction with the surface *d* states and a dispersed band is originated between –2.0 and –6.0 eV. The C=C COOP curves of analyzed η_3 and η_4 -cis

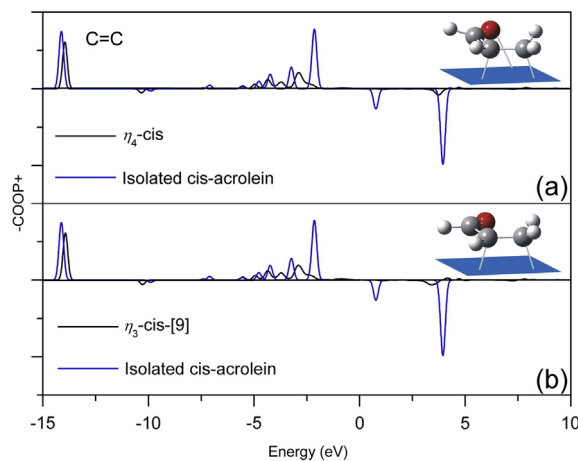


Fig. 4. Crystal orbital overlap population (COOP) curves of C=C bond in selected configurations during adsorption process of acrolein on a Pt (111) surface. (a) η_4 -cis obtained in the present study. (b) η_3 -cis proposed by Loffreda et al. [9].

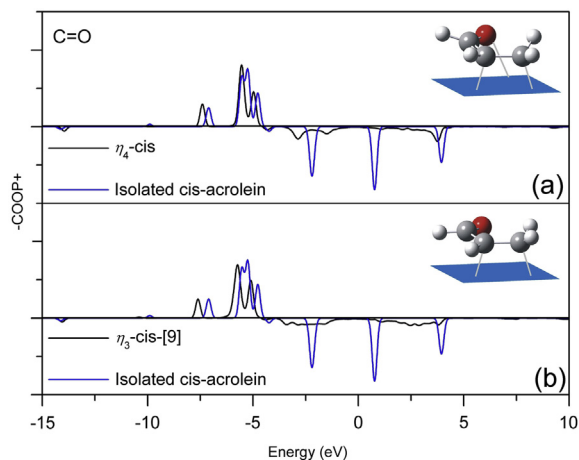


Fig. 5. Crystal orbital overlap population (COOP) curves of C=O bond in selected configurations during adsorption process of acrolein on a Pt (111) surface. (a) η_4 -cis obtained in the present study. (b) η_3 -cis proposed by Loffreda et al. [9].

configurations are very similar, in agreement with their comparable OP value (C=C %OP, $\sim -32.9\%$). Finally, Fig. 5(a) and (b) shows the COOP curves corresponding to the C=O bond. It can be seen that our η_4 -cis form presents a wide antibonding area below the Fermi level (between ~ -1.25 and -5 eV), which explains the higher weakening of the C=O overlap (-17.0% , see Table 3) in comparison with that evaluated in the η_3 -cis geometry proposed by Loffreda et al. (-12.0%) [9].

3.3. Density of states

Fig. 6 shows the electronic structure for the η_4 -cis form, the most stable acrolein bonding configuration on Pt (111). The black tick marks represent the electronic levels of isolated acrolein before adsorption. No adsorbate–adsorbate interaction was found due to the very low coverage. The DOS curve for the chemisorbed molecule shows bands spread out and enlarged as the result of the interaction between acrolein and metal states, especially with the d -orbitals. Acrolein states also shift to lower energies, so a stabilization of these orbitals takes place after adsorption. Similar orbital dispersion was obtained for the η_3 -cis configuration proposed by Loffreda et al. [9], however, our η_4 -cis geometry presents a more intense band in the region between 2.5 and 6 eV, which indicates a higher stability on the Pt surface. Fig. 7 shows the main orbital contributions to the DOS curves before and after η_4 -cis mode adsorption. When C p

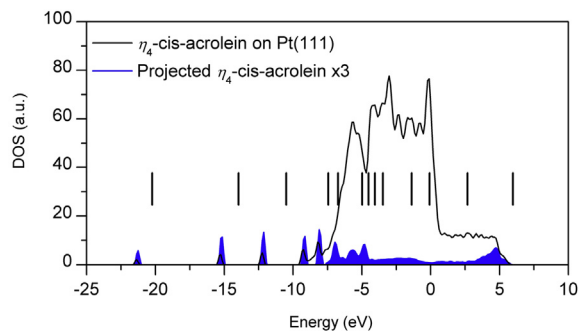


Fig. 6. Total DOS curves. η_4 -cis adsorption geometry obtained in the present study. The tick marks indicate the cis acrolein molecular orbitals before adsorption. In addition the projections of adsorbed acrolein DOS are shaded in blue. (For interpretation of the references to color in this figure legend, the reader is referred to the web version of this article.)

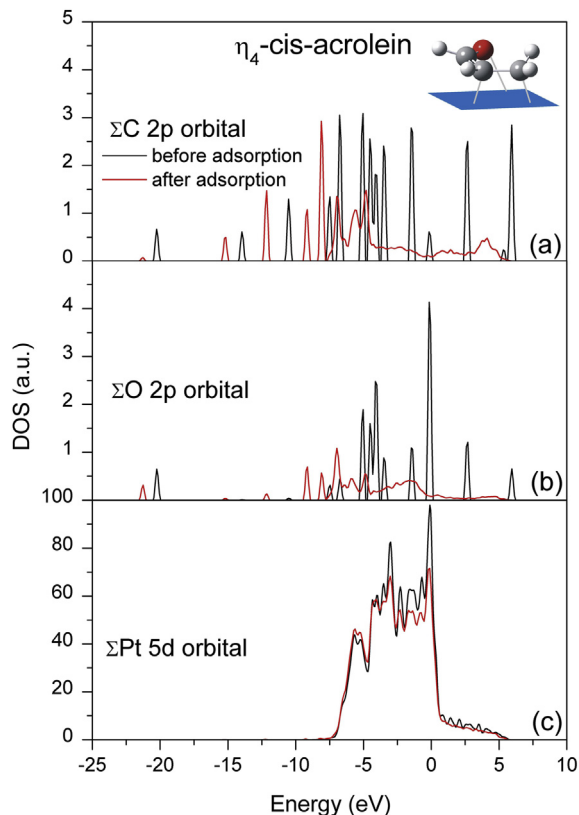


Fig. 7. Orbital contributions to DOS curves before and after η_4 -cis acrolein adsorption on a Pt (111) surface. (a) 2p orbital contribution from the three C atoms. (b) 2p orbital contribution from O atom. (c) 5d orbital contribution from the Pt atoms.

orbitals (Fig. 7(a)) and O p orbital (Fig. 7(b)) interact with the Pt surface, their DOS curves are extended over a 15 eV range. Regarding the contribution of Pt d orbitals (see Fig. 7(c)), a shift to lower energies after adsorption is not detected what differs from our previous calculations [10]. A fraction of the d -band goes across the Fermi level, indicating a stabilizing interaction. The changes from -7.5 to 6 eV suggest strong interactions between C and O p orbitals with Pt d states, while s contributions are limited.

Finally, the H, C, O and Pt orbital occupation changes during the acrolein adsorption are listed in Table 4. An important decrease in the Pt p_z and d_z^2 orbital populations are achieved in all cases, while the olefinic and saturated C p_z occupations increase, especially for the η_4 -cis configuration. These states play a main role in the bonding process, because the lobes of the C p_z orbitals are perpendicular to the surface and are well oriented to overlap with the Pt p_z and d_z^2 orbitals. The O p_x occupation decreases after chemisorption except for the η_1 -trans mode, whose major interaction occurs through its O p_z orbital. H s states do not have relevant contributions since their occupations change slightly after acrolein adsorption.

Table 4
Percentage of atomic orbital occupation for acrolein adsorption.

Atom	Orbital	Acrolein/Pt (111)						
		η_1 -trans	η_2 -cis	η_2 -trans	η_3 -cis	η_3 -trans	η_4 -cis	η_4 -trans
C1	$2p_z$	64.6	17.5	9.2	45.2	6.9	65.3	9.9
C3	$2p_z$	19.5	25.6	26.3	26.5	25.7	27.5	25.9
O1	$2p_x$	6.0	-3.2	-0.7	-5.0	-0.7	-5.1	-1.4
Pt	$6p_z$	-27.4	-15.4	-14.8	-32.4	-15.0	-28.8	-13.8
Pt	$5d_z^2$	-42.2	-29.6	-28.7	-37.5	-28.6	-39.8	-28.0

4. Conclusions

The adsorption of acrolein on a Pt (111) surface was studied by total energy calculation bonding analyses. The interatomic distances and bonding angles obtained for the final trans adsorption modes are in agreement with those previously reported [7,9], but our final adsorbed cis geometries are different. Our energetic study suggests that all the cis isomers have a similar stability on the Pt surface and the trans modes are less stable, in agreement with experimental (RAIRS) observations. Discrepancies with earlier calculations, which indicate that the most stable adsorption configuration is only the η_3 -cis, could be explained by means of differences in the k -point sampling. The inclusion of vdW dispersion forces provides better adsorption energies but does not change the adsorption geometry, site preference or relative energy values for all configurations. The COOP and OP analysis indicate that acrolein adsorption occurs via the formation of =C–Pt bonds, involving the two olefinic carbons. The η_4 -cis configuration, the most stable bonding structure on Pt (111), also shows very important –C–Pt and =O–Pt OP values. In addition, we found that the p_z orbitals of the three acrolein C atoms participates strongly in the adsorption process, as well as Pt p_z and d_z^2 orbitals.

Acknowledgments

The authors acknowledge SGCyT (UNS), CONICET, Departamento de Física (UNS), Departamento de Química (UNS), PICT 1770 and 1609 for financial support. All authors are members of CONICET.

References

- [1] Beccat P, Bertolini JC, Gauthier Y, Massardier J, Ruiz P. *J Catal* 1990;126:451–6.
- [2] Gallezot P, Richard D. *Catal Rev Sci Eng* 1998;40:81–126.
- [3] Marinelli TBLW, Nabuurs S, Ponc V. *J Catal* 1995;151:431–8.
- [4] de Jesús JC, Zaera F. *J Mol Catal A: Chem* 1999;138:237–40.
- [5] Claus P. *Top Catal* 1998;5:51–62.
- [6] Jesús JC, Zaera F. *Surf Sci* 1999;430:99–115.
- [7] Delbecq F, Sautet P. *J Catal* 2002;211:398–406.
- [8] Delbecq F, Sautet P. *J Catal* 1995;152:217–36.
- [9] Loffreda D, Jugnet Y, Delbecq F, Bertolini JC, Sautet P. *J Phys Chem B* 2004;108:9085–93.
- [10] Pirillo S, López-Corral I, Germán E, Juan A. *App Surf Sci* 2012;263:79–85.
- [11] Kresse G, Hafner J. *Phys Rev B* 1994;49:14251–69.
- [12] Kresse G, Hafner J. *Phys Rev B* 1993;47:558–61.
- [13] Grimme S. *J Comput Chem* 2004;25:1463–73.
- [14] Monkhorst HJ, Pack JD. *Phys Rev B* 1976;13:5188–92.
- [15] Deb B, editor. *The Hellmann–Feynman theorem, in the force concept in chemistry*. Toronto: Van Nostran–Reinhold; 1981.
- [16] Bader RFW. *Atoms in molecules—a quantum theory*. Oxford: Oxford University Press; 1990.
- [17] Henkelman G, Arnaldsson A, Jónsson H. *Comput Mater Sci* 2006;36:254–360.
- [18] Ordejón P, Artacho E, Soler JM. *Phys Rev B* 1996;53:R10441–4.
- [19] Soler JM, Artacho E, Gale JD, García A, Junquera J, Ordejón P, et al. *J Phys Condens Matter* 2002;14:2745–79.
- [20] Hoffmann R. *Solids and surfaces: a chemist's view of bonding in extended structures*. New York: VCH; 1988.
- [21] Edith Chan AW, Hoffmann R. *J Chem Phys* 1990;92:699–708.
- [22] Liu W, Carrasco J, Santra B, Michaelides A, Scheffler M, Tkatchenko A. *Phys Rev B* 2012;86:1–6. 245405.
- [23] Carrasco J, Klimeš J, Michaelides A. *J Chem Phys* 2013;138:1–9. 024708.
- [24] Ferullo R, Branda MM, Illas F. *J Phys Chem Lett* 2010;1:2546–9.
- [25] Hanke F, Dyer MS, Björk J, Persson M. *J Phys Condens Matter* 2012;24:1–9. 424217.
- [26] Tonigold K, Grob A. *J Chem Phys* 2010;132:1–10. 224701.
- [27] Yang B, Wang D, Gong X-Q, Hu P. *Phys Chem Chem Phys* 2011;13:21146–52.
- [28] Kang G-J, Jing M, Chen Z-X. *Catal Lett* 2012;142:287–93.